Atmos. Meas. Tech. Discuss., 7, 6287–6298, 2014
www.atmos-meas-tech-discuss.net/7/6287/2014/
doi:10.5194/amtd-7-6287-2014

Atmospheric Measurement Techniques Discussions
Open Access

Fiber optic distributed temperature sensing for the determination of air temperature

S. A. P. de Jong, J. D. Slingerland, and N. C. van de Giesen

Faculty of Civil Engineering and Geosciences, Delft University of Technology, Delft, the Netherlands

Received: 29 April 2014 – Accepted: 15 June 2014 – Published: 23 June 2014

Correspondence to: N. C. van de Giesen (n.c.vandegiesen@tudelft.nl)

Published by Copernicus Publications on behalf of the European Geosciences Union.

Abstract

This paper describes a method to correct for the effect of solar radiation in atmospheric Distributed Temperature Sensing (DTS) applications. By using two cables with different diameters, one can determine what temperature a zero diameter cable would have. Such virtual cable would not be affected by solar heating and would take on the temperature of the surrounding air. The results for a pair of black cables and a pair of white cables were very good. The correlations between standard air temperature measurements and air temperatures derived from both colors had a high correlation coefficient ($r^2 = 0.99$). A thin white cable measured temperatures that were close to air temperature. The temperatures were measured along horizontal cables but the results are especially interesting for vertical atmospheric profiling.

1 Introduction

Distributed Temperature Sensing (DTS) is a technique that allows for measurement of temperature along optical fibers. Laser pulses are shot into the fiber and backscatter from within the fiber is analyzed. The time of flight then gives the position along the fiber from where the backscatter originated. Analysis of the Raman spectrum of the backscatter allows for the calculation of the temperature at the place where the backscatter originated. Depending on the type of DTS machine used, temperatures can be measured continuously at sub-meter intervals along cables of more than 5 km, with accuracies up to 0.01 °C. A good introduction to DTS principles and environmental applications can be found in Selker et al. (2006) and Tyler et al. (2009).

Over the past decade, DTS has found many environmental applications. Applications vary from temperature profiling of the subsurface (borehole observations, Freifeld et al., 2008, soils, Jansen et al., 2011; Sayde et al., 2010; Steele-Dunne et al., 2010), water (estuaries, Henderson et al., 2009, surface/groundwater, Lowry et al., 2007; Mamer and Lowry, 2013, solar ponds, Suárez et al., 2011, streams, Selker et al., 2006;

Vogt et al., 2010; Westhoff et al., 2007, 2011 and lakes, Vercauteren et al., 2011; van Emmerik et al., 2013), rocks (Read et al., 2013), ice caves (Curtis and Kyle, 2011), forests (Krause et al., 2013) and infrastructure (dam surveillance, Dornstadter, 1998, sewers, Hoes et al., 2009, electric transmission cables, Yilmaz and Karlik, 2006 and gas pipelines, Tanimola and Hill, 2009).

There are only a few experiments where DTS is used to measure atmospheric temperature (Keller et al., 2011; Petrides et al., 2011; Thomas et al., 2012), since solar heating can have a significant effect. Keller et al. (2011) experimented during night time to exclude the effect of short-wave radiation. Petrides et al. (2011) estimates effective shade and concluded that solar radiation is the driving factor in temperature differences. Thomas et al. (2012) observed differences in temperature measurements with black and white cables and suggests that it can be used for setting up an energy balance.

This paper will describe a method to correct for the effect of solar radiation in atmospheric DTS measurements with the use of fiber optic cables with different diameters.

2 Materials and methods

2.1 Theory

Solar radiation causes objects to be warmer than the surrounding air. For this reason, thermometers are traditionally shielded by a Stevenson screen. The temperature difference between a solar heated cylinder (or sphere) and the air that moves around it, scales with the square root of the diameter (White, 1988). If the diameter of a cylinder would be zero, the heat generated by solar radiation would also be zero. Such a zero diameter cylinder would take on the temperature of the surrounding air. One can create a virtual cylinder with zero diameter by extrapolating the temperatures of two cylinders with different diameters. The theory behind this idea, which was first put forward by Gaylon Campbell, assumes an infinitely long cylinder, instant redistribution

AMTD
7, 6287–6298, 2014

of heat within a cross-section of the cylinder, and forced convection on the outside of the cylinder. Forced convection dominates when the buoyancy force parameter, also known as the Archimedes number, Ar, is much smaller than one. For a cylinder of diameter d (m) we have:

$$Ar = \frac{Gr}{Re^2} = g \times \frac{T_s - T_{air}}{T_{air}} \times \frac{d}{v^2} \tag{1}$$

with Gr the Grashof number (–), Re the Reynolds number (–), g the acceleration due to gravity (9.8 m s^{-2}), T_{air} the air temperature (K), T_s the surface temperature of the cable (K) and v the windspeed (m s^{-1}).

When the temperatures of two cables (T_1 and T_2) with different diameters (d_1 and d_2) are measured, then the air temperature can be determined with Eq. (2).

$$T_{air} = T_2 - \frac{T_1 - T_2}{\sqrt{\frac{d_1}{d_2}} - 1} \tag{2}$$

2.2 Experimental setup

The measurements were taken from 27 April 2011 through 3 May 2011 on a grass field near Delft University of Technology, Delft, The Netherlands (51°59′45.44″ N, 42°2′39.56″ E). The DTS instrument was a HALO unit (Sensornet, Elstree, UK) with a sampling interval of 2 m and a measurement interval of 20 s. The fiber optic cables used in this experiment consisted of single (simplex) multi-mode, bend insensitive, optical fibers, tight packed, protected with Kevlar and a plastic jacket (AFL, South Carolina, USA).

A schematic drawing of the experimental setup is shown in Fig. 1. The cable consisted of four sections, one black with diameter 3.0 mm, one black with diameter 1.6 mm, one white with diameter 3.0 mm and one white with diameter 1.6 mm. Each section had a length of 190 m. The sections were fused together to enable continuous measurements.

AMTD
7, 6287–6298, 2014

The fiber was measured in a single-ended configuration. For calibration purposes, each section had 20 m of fiber cable coiled up in a thermally insulated water bath with warm water (average 27 °C) and cold water (average 14 °C). Calibration of the fiber optic cable was based on the method described by Hausner et al. (2011). Of each section, 150 m of fiber optic cable was held in open air, 1 m above the grass, with the use of pigtail fence posts.

For this analysis, the 75 measurement points of each section hanging in the air were averaged to one time series. To improve the signal to noise ratio, the DTS measurements were averaged over time using an integration time of five minutes. We assume that heat within the cross section of the cable is distributed equally at this time scale.

As a reference station, a HOBO weather station (Onset Computer Corporation, USA) with rain (mm), temperature (°C), relative humidity (%) and incoming solar radiation ($W\,m^{-2}$) was installed next to the experimental setup. The temperature/RH sensor used was a 12-bit Temperature Smart Sensor (S-THB-M002) with a reported accuracy of ±0.13 °C. The reference station had a measurement interval of 5 min.

Wind velocity data, to determine if the assumption of forced convection was valid, was taken from the closest automated weather station of the Royal Netherlands Meteorological Institute. This station is situated at the airport of Rotterdam (51°57′33.66″ N, 4°26′32.66″ E), 6 km from the experiment location.

3 Results and discussion

Weather conditions from 27–30 April were partly cloudy with a daily maximum incoming solar radiation between 600–650 $W\,m^{-2}$. On 28 April there was a rain event with 2.4 mm of rain. Conditions from 1–3 May were clear and sunny with daily maximum incoming solar radiation between 650–750 $W\,m^{-2}$.

The dominant wind direction was North-East. The wind speed during daytime varied between 3–9 $m\,s^{-1}$, making the assumption of forced convection valid ($Ar < 0.001$). Note that forced convection will dominate in all but the most extreme natural conditions.

AMTD
7, 6287–6298, 2014

Figure 2 shows the average temperature measured by, respectively, the black cables and the white cables. The uncorrected temperatures show a clear temperature rise during daytime due to solar heating. This effect is significantly larger for the black cables than for the white cables. During daytime, the black cables show a clear temperature rise due to solar heating. The correlation coefficient r^2, see Fig. 3, between the uncorrected temperature of the black 3.0 mm and 1.6 mm cable with the reference station is respectively $r^2 = 0.77$ and $r^2 = 0.85$ and a RMSE of 2.40 °C and 1.80 °C. The uncorrected temperature of the white 3.0 and 1.6 mm cable show a correlation of respectively $r^2 = 0.97$ and $r^2 = 0.98$ and a RMSE of 0.74 °C and 0.61 °C. The corrected temperatures of both the white and black cable have a r^2 of 0.99 and a RMSE of 0.38 °C.

4 Conclusions

Distributed Temperature Sensing (DTS) of atmospheric temperature profiles is hindered by solar heating, which may lead to significant deviations from the true air temperature. For atmospheric measurements with DTS we showed that it is possible to correct for solar heating and find a good estimation for the air temperature, by using cables with different diameters.

The corrected temperatures closely matched the temperature measurements of the reference station. The method used to calculate the air temperature is independent of the color of the cable. If it is not possible to apply different sizes of cable in a setup in an atmospheric DTS application, the use of a thin white fiber optic cable is a reasonably good alternative. This method will be especially valuable for vertical atmospheric soundings with DTS from balloons, quadcopters, or towers.

AMTD
7, 6287–6298, 2014

References

Curtis, A. and Kyle, P.: Geothermal point sources identified in a fumarolic ice cave on erebus volcano, antarctica using fiber optic distributed temperature sensing, Geophys. Res. Lett., 38, L16802, doi:10.1029/2011GL048272, 2011. 6289

Dornstadter, M. and Aufleger, D.: The prospect for reservoirs in the 21st century, in: Proceedings of the Tenth Conference of the BDS Held at the University of Wales, Bangor, 9–12 September 1998, Thomas Telford Publishing, 1998. 6289

Freifeld, B. M., Finsterle, S., Onstott, T. C., Toole, P., and Pratt, L. M.: Ground surface temperature reconstructions: using in situ estimates for thermal conductivity acquired with a fiber-optic distributed thermal perturbation sensor, Geophys. Res. Lett., 35, L14309, doi:10.1029/2008GL034762, 2008. 6288

Hausner, M. B., Suárez, F., Glander, K. E., Van de Giesen, N., Selker, J. S., and Tyler, S. W.: Calibrating single-ended fiber-optic raman spectra distributed temperature sensing data, Sensors, 11, 10859–10879, doi:10.3390/s111110859, 2011. 6291

Henderson, R. D., Day-Lewis, F. D., and Harvey, C. F.: Investigation of aquifer-estuary interaction using wavelet analysis of fiber-optic temperature data, Geophys. Res. Lett., 36, L06403, doi:10.1029/2008GL036926, 2009. 6288

Hoes, O., Schilperoort, R., Luxemburg, W., Clemens, F., and Van de Giesen, N.: Locating illicit connections in storm water sewers using fiber-optic distributed temperature sensing, Water Res., 43, 5187–5197, doi:10.1016/j.watres.2009.08.020, 2009. 6289

Jansen, J., Stive, P., Van de Giesen, N., Tyler, S., Steele-Dunne, S., and Williamson, L.: Estimating soil heat flux using distributed temperature sensing, IAHS Publ., 343, 140–144, 2011. 6288

Keller, C. A., Huwald, H., Vollmer, M. K., Wenger, A., Hill, M., Parlange, M. B., and Reimann, S.: Fiber optic distributed temperature sensing for the determination of the nocturnal atmospheric boundary layer height, Atmos. Meas. Tech., 4, 143–149, doi:10.5194/amt-4-143-2011, 2011. 6289

Krause, S., Taylor, S. L., Weatherill, J., Haffenden, A., Levy, A., Cassidy, N. J., and Thomas, P. A.: Fibre-optic distributed temperature sensing for characterizing the impacts of vegetation coverage on thermal patterns in woodlands, Ecohydrology, 6, 754–764, doi:10.1002/eco.1296, 2013. 6289

Lowry, C. S., Walker, J. F., Hunt, R. J., and Anderson, M. P.: Identifying spatial variability of groundwater discharge in a wetland stream using a distributed temperature sensor, Water Resour. Res., 43, W10408, doi:10.1029/2007WR006145, 2007. 6288

Mamer, E. A. and Lowry, C. S.: Locating and quantifying spatially distributed groundwater-surface water interactions using temperature signals with paired fiber-optic cables, Water Resour. Res., 49, 7670–7680, doi:10.1002/2013WR014235, 2013. 6288

Petrides, A. C., Huff, J., Arik, A., Van de Giesen, N., Kennedy, A. M., Thomas, C. K., and Selker, J. S.: Shade estimation over streams using distributed temperature sensing, Water Resour. Res., 47, W07601, doi:10.1029/2010WR009482, 2011. 6289

Read, T., Bour, O., Bense, V., Le Borgne, T., Goderniaux, P., Klepikova, M., Hochreutener, R., Lavenant, N., and Boschero, V.: Characterizing groundwater flow and heat transport in fractured rock using fiber-optic distributed temperature sensing, Geophys. Res. Lett., 40, 2055–2059, doi:10.1002/grl.50397, 2013. 6289

Sayde, C., Gregory, C., Gil-Rodriguez, M., Tufillaro, N., Tyler, S., Van de Giesen, N., English, M., Cuenca, R., and Selker, J. S.: Feasibility of soil moisture monitoring with heated fiber optics, Water Resour. Res., 46, W06201, doi:10.1029/2009WR007846, 2010. 6288

Selker, J., Van de Giesen, N., Westhoff, M., Luxemburg, W., and Parlange, M. B.: Fiber optics opens window on stream dynamics, Geophys. Res. Lett., 33, L24401, doi:10.1029/2006GL027979, 2006. 6288

Steele-Dunne, S. C., Rutten, M. M., Krzeminska, D. M., Hausner, M., Tyler, S. W., Selker, J., Bogaard, T. A., and Van de Giesen, N. C.: Feasibility of soil moisture estimation using passive distributed temperature sensing, Water Resour. Res., 46, W03534, doi:10.1029/2009WR008272, 2010. 6288

Suárez, F., Aravena, J. E., Hausner, M. B., Childress, A. E., and Tyler, S. W.: Assessment of a vertical high-resolution distributed-temperature-sensing system in a shallow thermohaline environment, Hydrol. Earth Syst. Sci., 15, 1081–1093, doi:10.5194/hess-15-1081-2011, 2011. 6288

Tanimola, F. and Hill, D.: Distributed fibre optic sensors for pipeline protection, Journal of Natural Gas Science and Engineering, 1, 134–143, doi:10.1016/j.jngse.2009.08.002, 2009. 6289

Thomas, C., Kennedy, A., Selker, J., Moretti, A., Schroth, M., Smoot, A., Tufillaro, N., and Zeeman, M.: High-resolution fibre-optic temperature sensing: A new tool to study the two-dimensional structure of atmospheric surface-layer flow, Bound.-Lay. Meteorol., 142, 177–192, 2012. 6289

Tyler, S. W., Selker, J. S., Hausner, M. B., Hatch, C. E., Torgersen, T., Thodal, C. E., and Schladow, S. G.: Environmental temperature sensing using raman spectra dts fiber-optic methods, Water Resour. Res., 45, W00D23, doi:10.1029/2008WR007052, 2009. 6288

Van Emmerik, T., Rimmer, A., Lechinsky, Y., Wenker, K., Nussboim, S., and Van de Giesen, N.: Measuring heat balance residual at lake surface using distributed temperature sensing, Limnol. Oceanogr.-Meth., 11, 79–90, 2013. 6289

Vercauteren, N., Huwald, H., Bou-Zeid, E., Selker, J. S., Lemmin, U., Parlange, M. B., and Lunati, I.: Evolution of superficial lake water temperature profile under diurnal radiative forcing, Water Resour. Res., 47, W09522, doi:10.1029/2011WR010529, 2011. 6289

Vogt, T., Schneider, P., Hahn-Woernle, L., and Cirpka, O. A.: Estimation of seepage rates in a losing stream by means of fiber-optic high-resolution vertical temperature profiling, J. Hydrol., 380, 154–164, doi:10.1016/j.jhydrol.2009.10.033, 2010. 6289

Westhoff, M. C., Savenije, H. H. G., Luxemburg, W. M. J ., Stelling, G. S., van de Giesen, N. C., Selker, J. S., Pfister, L., and Uhlenbrook, S.: A distributed stream temperature model using high resolution temperature observations, Hydrol. Earth Syst. Sci., 11, 1469–1480, doi:10.5194/hess-11-1469-2007, 2007. 6289

Westhoff, M. C., Gooseff, M. N., Bogaard, T. A., and Savenije, H. H. G.: Quantifying hyporheic exchange at high spatial resolution using natural temperature variations along a first-order stream, Water Resour. Res., 47, W10508, doi:10.1029/2010WR009767, 2011. 6289

White, F.: Heat and Mass Transfer, Addison-Wesley series in mechanical engineering, Addison Wesley Publishing Company Incorporated, 1988. 6289

Yilmaz, G. and Karlik, S. E.: A distributed optical fiber sensor for temperature detection in power cables, Sensor. Actuat. A-Phys., 125, 148–155, doi:10.1016/j.sna.2005.06.024, 2006. 6289

AMTD

7, 6287–6298, 2014

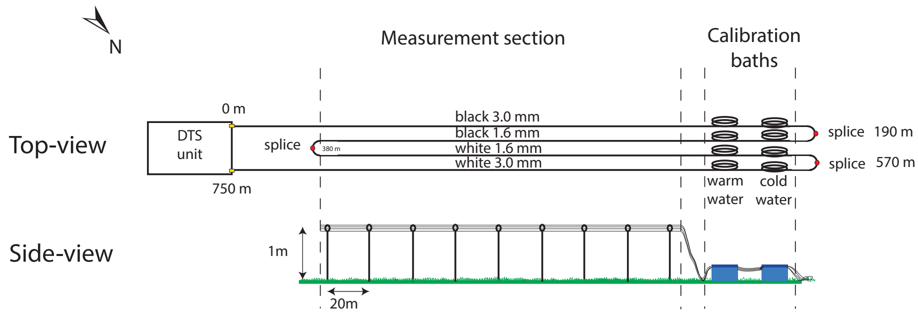

Figure 1. Schematic overview of the experimental setup. The cable consisted of four sections (black with diameter 3.0 mm and 1.6 mm and white with diameter 3.0 mm and 1.6 mm). In the measurement section the cables are held in open air above a grass field.

AMTD
7, 6287–6298, 2014

Determination of air temperature with DTS

S. A. P. de Jong et al.

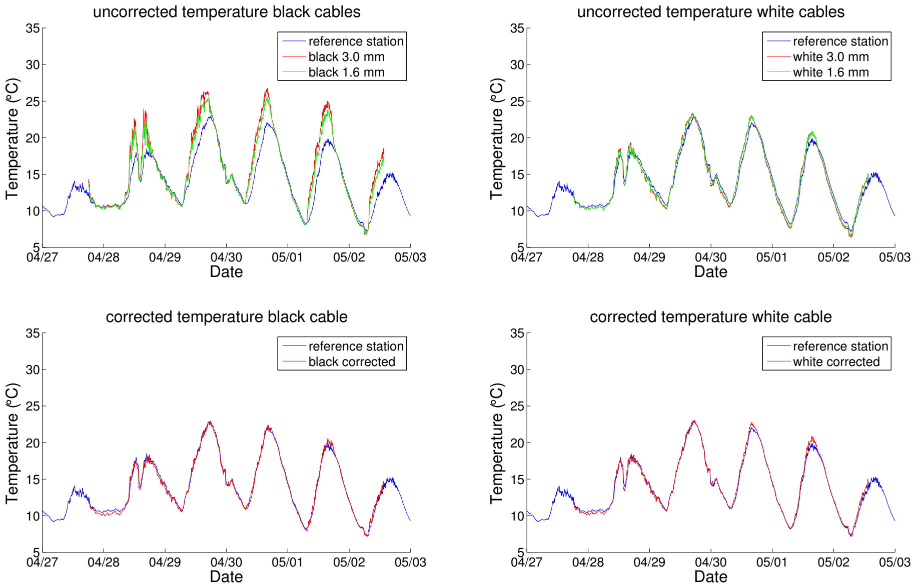

Figure 2. Top: comparison between the reference station and the uncorrected averaged temperature of the black (left) and white (right) cables in the measurement section. Bottom: comparison between the reference station and the corrected temperatures of the black (left) and white (right) cable.

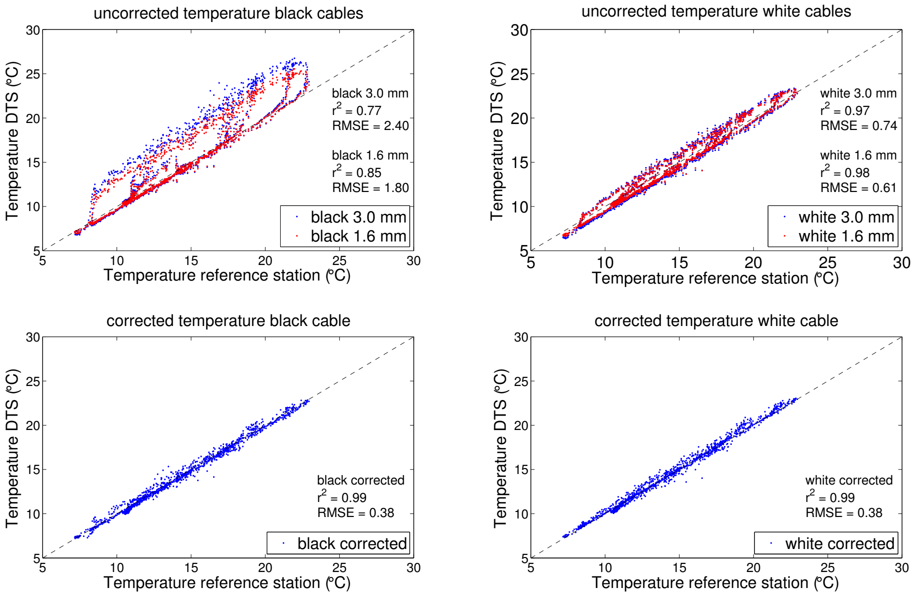

Figure 3. Top: correlations between the temperature measurements of the reference station and the uncorrected temperatures of the black (left) and white (right) cable. Bottom: correlation between the temperature measurements of the reference station and the corrected temperatures of the black (left) and white (right) fiber optic cables.